

N 65-35284

FACILITY FORM 802

(ACCESSION NUMBER)

13

(PAGES)

(THRU)

(CODE)

(NASA CR OR TMX OR AD NUMBER)

(CATEGORY)

## PRELIMINARY RESULTS OF BOUNDARY-LAYER NOISE

MEASURED ON THE X-15 AIRPLANE

By Eldon E. Kordes and Carole S. Tanner

NASA Flight Research Center  
Edwards, Calif.

GPO PRICE \$ \_\_\_\_\_

CSFTI PRICE(S) \$ \_\_\_\_\_

Hard copy (HC) 1.00Microfiche (MF) .50

ff 653 July 65

Second International Conference on Acoustical Fatigue  
Dayton, Ohio  
April 29 to May 1, 1964

May 1, 1964

# PRELIMINARY RESULTS OF BOUNDARY-LAYER NOISE

## MEASURED ON THE X-15 AIRPLANE

By Eldon E. Kordes and Carole S. Tanner

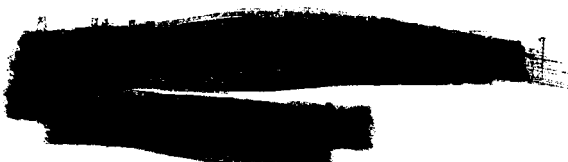
NASA Flight Research Center  
Edwards, Calif.

### INTRODUCTION

The fluctuating pressures that generate noise in the boundary layer and the effects of this acoustic energy on panel response, panel fatigue, and internal sound levels are of continuing concern to the designers of high-speed flight vehicles. Theoretical analysis and experimental studies using model jets, aircraft, and missiles have been conducted to define the physical quantities governing the intensity and frequency content of boundary-layer noise (refs. 1 to 4, for example). Most of the flight-test data have been limited to Mach numbers less than 2.5 (refs. 1 and 2), although the Scout missile has gathered boundary-layer-noise data at Mach numbers up to 4 (ref. 3) and the Project Mercury vehicles (ref. 4) up to Mach 5.7. These flight-test data have been extremely valuable; however, all data obtained on flight vehicles at Mach numbers of 3 and above have been for highly transient flight conditions which requires compromise in the analysis for the effects of various flight parameters.

In order to provide detailed information on boundary-layer noise over a wide range of controlled flight conditions, the NASA Flight Research Center is conducting a boundary-layer-noise research program with the X-15 airplane. This paper describes the program and presents some of the preliminary results.

The X-15 airplane has performance capabilities that make it useful in obtaining boundary-layer-noise data for Mach numbers up to 6 and dynamic pressures up to 1,500 psf. During flight, many of the conditions can be held essentially constant long enough to obtain excellent data samples, and data can be obtained in both the acceleration and the deceleration phases. The X-15 instrument package is completely recoverable and can be calibrated before and after each flight or modified as required. The shaded area in figure 1 shows the X-15 flight envelope available for boundary-layer-noise studies. Only the portion of the X-15 flight envelope for dynamic pressures above 100 psf and altitudes below 150,000 feet is shown. For dynamic pressures of 1,500 psf, the flight-test Mach number range extends to slightly greater than 5. For dynamic pressures of 500 psf or less, the vehicle is capable of flight to a Mach number of 6.



## INSTRUMENTATION

It would be desirable to measure boundary-layer noise at many locations in order to study the effects of local flow for different boundary conditions. On the X-15, however, only a limited number of areas are available without modification to the basic airframe. The X-15 side fairings were constructed of access panels for servicing wiring, hydraulic lines, and control cables. Four specific panels on the original X-15 side-fairing surfaces have been modified for the boundary-layer-noise studies (fig. 2). The preliminary data presented in this paper were obtained from the lower test panel on the right side of the aircraft, just behind the wing leading edge.

The test-panel instrumentation is illustrated in figure 3. Two crystal microphones are flush-mounted in a block at the front of the panel. The sectional view shows the microphones in their mounting block and a uniaxial accelerometer attached to the back of the mounting block. The noise-measuring microphone is shown on the right. The dummy microphone on the left measures the temperature environment of the diaphragm and the crystal. This dummy microphone is required for defining the temperatures, since it is not possible to instrument the active microphone. Immediately behind the microphones is a test area with a removable panel. After the boundary layer has been defined, a study of the response of different structures to boundary-layer noise is planned. Aft of the response panel is a boundary-layer rake with 12 total-pressure-measuring stations.

All of the data, except temperature, from the microphones, accelerometer, and boundary-layer rake are recorded on an onboard tape recorder. Figure 4 illustrates the schematic hookup of the data-recording system. The microphone and accelerometer signal outputs are amplified and recorded on separate channels of the tape recorder. The rake pressure transducer signal outputs are each fed to a voltage control oscillator box where they are multiplexed and recorded on the tape recorder. The dummy microphone thermocouple signal outputs are recorded on the onboard oscillograph.

## DATA REDUCTION

The methods of data analysis used in this program are illustrated by the block diagram of figure 5. For the noise analysis, the flight tape is played back and either a time history of overall sound pressure levels (OASPL) is obtained, or the noise is fed to a one-third octave-band analyzer and a time history of all the third octave bands from 50 cps to 10,000 cps is obtained. Specific portions of the flight data can be recorded on a tape loop and analyzed in third-octave-band spectrograms. The flight data on the tape loop vary from 5 seconds to 30 seconds, depending on the flight parameters selected. The pressure data are played back through a discriminator and recorded on oscillograph paper. Accelerometer data are played back directly to obtain the acceleration time history and then played through a frequency analyzer to obtain g-levels as a

function of frequency. The accelerometer data are used as a check on the microphone acceleration environment. The thermocouple data from the dummy microphone are read from the oscillograph film using standard film-reading equipment to obtain the temperature ( $^{\circ}\text{F}$ ) time history of the microphone diaphragm and crystal.

### SYSTEM RESPONSE

As might be expected, one of the major problems has been to obtain a microphone and a recorder that are capable of predictable response over a wide range of temperature, altitude, and accelerations. On the X-15 the effects of vibratory acceleration on the microphone output have not been a problem. The characteristics of systems used in this program are summarized in figure 6 in which typical pressure response of the microphone and recorder system is shown for several environmental conditions.

As shown in the top plot the complete system has an essentially constant response of  $-5\text{ db}^*$  over the frequency range from 50 cps to 10,000 cps at room temperature and local altitude (2,500 ft). In order to illustrate the effects of transient heating, the sensitivity change of the microphone with temperature is shown in the middle plot for a constant frequency of 1,000 cps. The microphone diaphragm was heated over the temperature profile from  $-40^{\circ}\text{F}$  to  $325^{\circ}\text{F}$  in 5 minutes, then allowed to cool. This temperature history is typical of those experienced on an X-15 flight. During the initial portion of heating shown in the figure, the erratic behavior of the microphone is attributed to thermal buckling of the diaphragm. Once the diaphragm and crystal arrive at a stable configuration, the microphone sensitivity change approaches zero with additional change in temperature. For microphone temperatures below  $75^{\circ}\text{F}$ , the data are considered to be unreliable. The bottom curve shows the effect of altitude on the sensitivity change of the microphone for a constant frequency of 1,000 cps. The sensitivity change is 2 db or less for altitudes up to 100,000 feet. Similar data have been obtained at other frequencies and heating rates. Results of this type are used to adjust the flight data and to indicate where improvements in the system are required.

### RESULTS AND DISCUSSION

No flights for the specific purpose of obtaining boundary-layer-noise data have been made thus far in the program. Equipment has been checked out and gross measurements of boundary-layer noise to be expected have been obtained on flights made for other general research purposes. During this preliminary portion of the program, acceptable boundary-layer-noise data have been obtained on only one flight. A time history of this flight is shown in figure 7. As can be seen, the four flight parameters are highly transient;

---

\*Referred to  $0.0002\text{ dynes/cm}^2$ .

only 5 to 10 seconds of near-steady-state conditions occurred in altitude, dynamic pressure, or Mach number. The angle of attack fluctuates greatly throughout the entire flight; however, flights made principally to obtain boundary-layer-noise measurements would be flown with much better control of angle of attack. The noise data measured on this flight were used to obtain a time history of overall sound pressure level and one-third octave band spectrograms for the near-steady-state Mach number at 210 to 220 seconds and for two values of dynamic pressure at 280 to 300 seconds and 320 to 335 seconds.

The overall sound pressure level measured on this flight is presented in figure 8 as a function of flight time. Data before the 170-second point have been omitted because of the erratic behavior of the microphones at the low temperature during the initial portion of the flight (see fig. 6). The maximum value of the overall sound pressure level measured on this flight is 147 db. The overall sound pressure level tends to follow the free-stream dynamic pressure except for a rather abrupt change in the sound pressure level at 250 seconds, when a large change occurred in airplane angle of attack. Although the angle-of-attack change does not affect the overall sound pressure level directly, an increase in angle of attack tends to compress the boundary layer on the lower surface of the vehicle and to introduce a crossflow around the cylindrical fuselage. These changes in the airflow at the measuring station would be expected to affect the overall sound pressure level. The data indicate that small variations in the angle of attack about an average value do not affect the noise levels. Changes in the overall sound pressure level at 270 seconds and at 365 seconds can be correlated with gross changes in the average angle of attack; however, no such correlation is evident at subsonic conditions.

Spectrograms of the boundary-layer noise at maximum Mach number and at the two portions of the flight with nearly constant dynamic pressure are shown in figure 9. The two upper curves are for different ranges of Mach number but for the same average angle of attack and approximately the same dynamic pressure. These two curves show about the same trends between 125 cps and 2,000 cps; the effect of Mach number appears to be evident only at the frequencies above 2,000 cps and below 125 cps. The fact that the solid curve lies below the other two curves at all frequencies is attributed to differences in the local flow conditions.

To show more clearly the differences in the boundary layer for the three portions of the flight analyzed for the data of figure 9, boundary-layer profiles obtained from the rake pressures are presented in figure 10. As can be seen, the region of maximum pressure gradient for the curve at  $M = 5.3$  and  $\alpha = 0^\circ$  is farther from the surface than the corresponding region at the lower Mach numbers and higher angles of attack. The results indicate that the nearer the region of maximum pressure gradient is to the surface, the higher the sound pressure level will be (ref. 5). Future efforts will be directed toward a better understanding of the factors affecting the local flow and their contribution to the boundary-layer noise.

In figure 8 there is an apparent relationship between sound-pressure level and dynamic pressure. This relationship has been noted previously by other investigators (ref. 3, for example). The ratio of surface pressure  $\sqrt{\frac{p}{p_\infty}}$

to the free-stream dynamic pressure  $q$  is plotted as a function of Mach number in figure 11. The solid curve for the X-15 is for both the climb and the descent. For comparison, data obtained on a Scout missile during the climb (ref. 3) are shown also. The angle of attack is essentially zero for the Scout during the entire flight and for the X-15 during climb from a Mach number of 3 to 5.3. For the Mach number range from 3.5 to 4, both vehicles have values of free-stream dynamic pressure in excess of 1,000 psf. As shown, the agreement of the data over this range of Mach numbers is excellent. The higher values of the surface-pressure coefficient for the X-15 during descent may be attributed to the effect of angle of attack, as mentioned previously. For Mach numbers from about 3.5 to 1.75, the average angle of attack was approximately  $4^\circ$ , and the values of the surface-pressure coefficient for the X-15 are approximately twice the values for the Scout. Even with the differences in the actual values of the pressure ratio, the trend with Mach number is similar for the two vehicles, that is, the surface-pressure coefficient decreases with an increase in Mach number up to 3.5.

#### CONCLUDING REMARKS

Preliminary data on boundary-layer noise obtained from an experimental program with the X-15 airplane show trends similar to data obtained on the Scout missile for comparable flight conditions. In addition, these data show that changes in the noise levels occur as a result of vehicle maneuvers at supersonic speeds. The X-15 program includes instrumentation for obtaining real-time information on the boundary-layer flow as well as boundary-layer noise. Future efforts will be directed toward a better understanding of the factors affecting the local flow and their contributions to the boundary-layer noise.

#### SYMBOLS

M	free-stream Mach number
P	total pressure, psf
$\sqrt{p^2}$	root-mean-square surface pressure, psf
q	free-stream dynamic pressure, psf
$\alpha$	angle of attack, deg

Subscript:

12 rake station 12

## REFERENCES

1. McLeod, Norman J., and Jordan, Gareth H.: Preliminary Flight Survey of Fuselage and Boundary-Layer Sound-Pressure Levels. NACA RM H58B11, 1958.
2. McLeod, Norman J.: Flight-Determined Aerodynamic-Noise Environment of an Airplane Nose Cone Up to a Mach Number of 2. NASA TN D-1160, 1962.
3. Hilton, David A., Bracalente, Emedio M., and Hubbard, Harvey H.: In-Flight Aerodynamic Noise Measurements on a Scout Launch Vehicle. NASA TN D-1818, 1963.
4. Mayes, William H., Hilton, David A., and Hardesty, Charles A.: In-Flight Noise Measurements for Three Project Mercury Vehicles. NASA TN D-997, 1962.
5. Lighthill, M. J.: On Sound Generated Aerodynamically. II: Turbulence As a Source of Sound. Proc. Roy. Soc. (London), ser. A, vol. 222, 1954, pp 1-32.

# X-15 FLIGHT ENVELOPE BOUNDARY-LAYER-NOISE PROGRAM

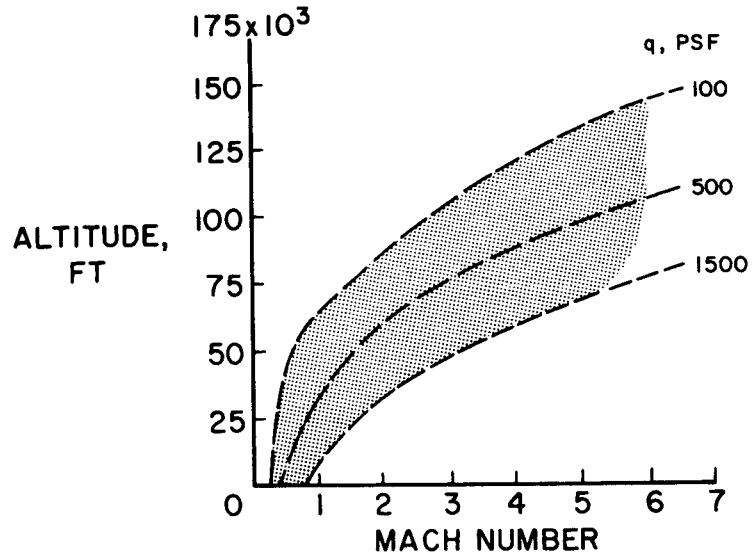


Figure 1

## X-15 BOUNDARY-LAYER-NOISE TEST PANELS

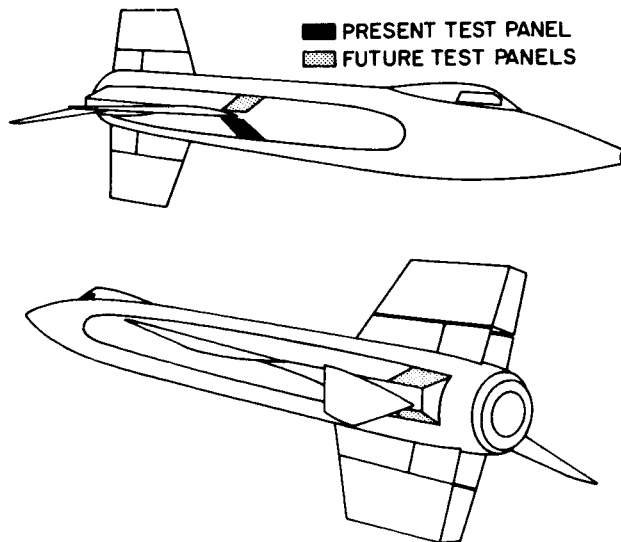


Figure 2



# BOUNDARY-LAYER-NOISE TEST PANEL

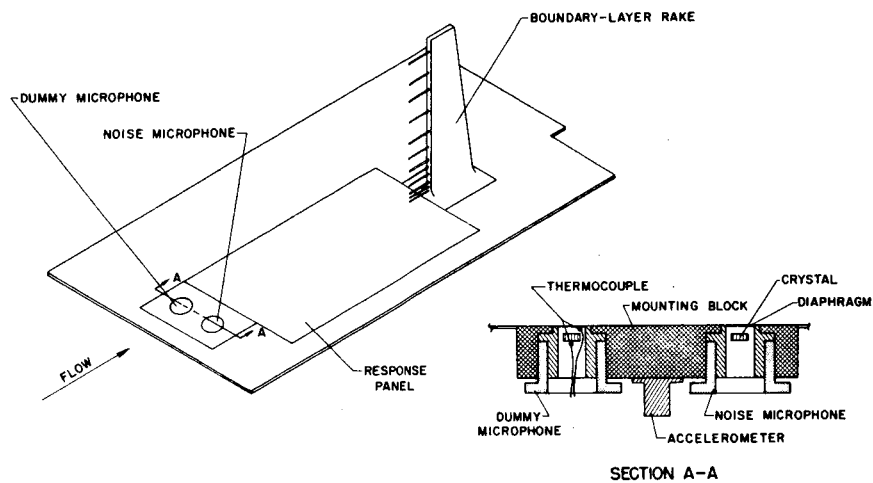


Figure 3

# DATA-RECORDING SYSTEM BOUNDARY-LAYER NOISE

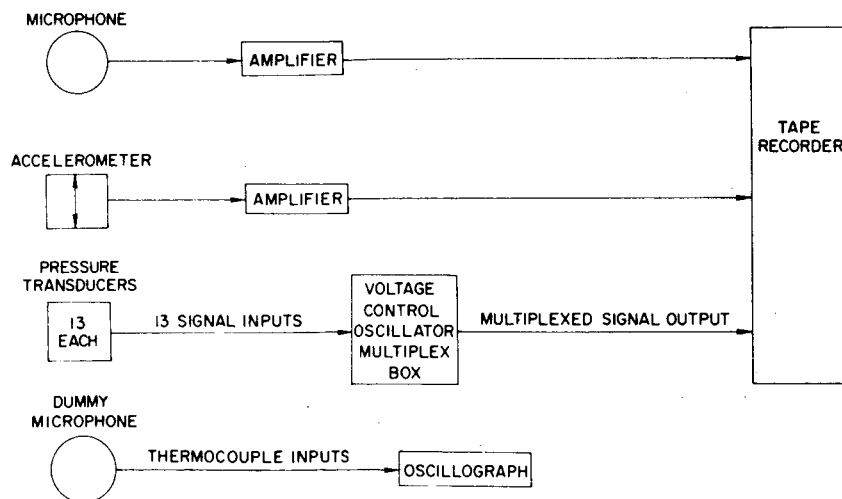


Figure 4

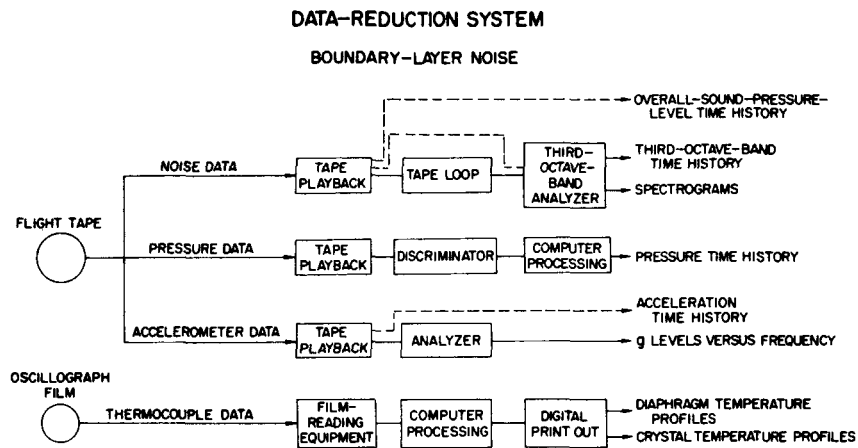


Figure 5

### TYPICAL RESPONSE CHARACTERISTICS

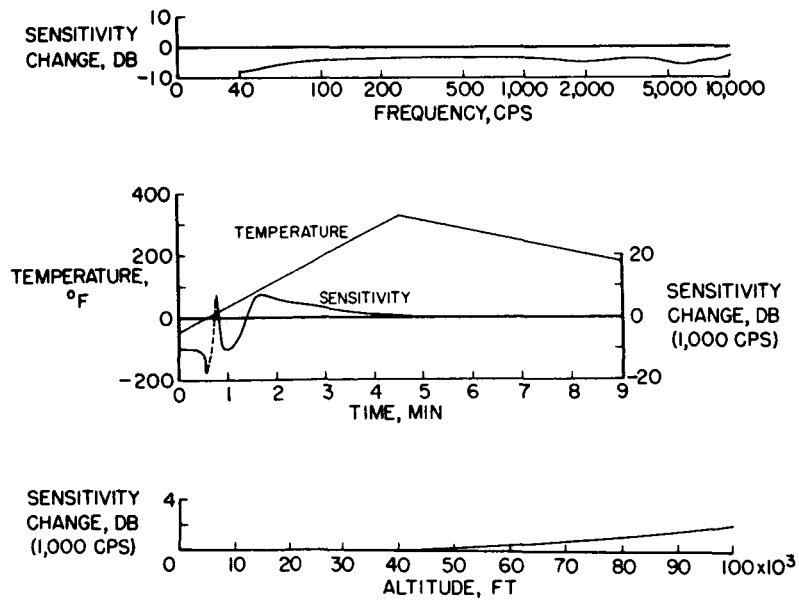


Figure 6

# X-15 FLIGHT HISTORY BOUNDARY-LAYER NOISE

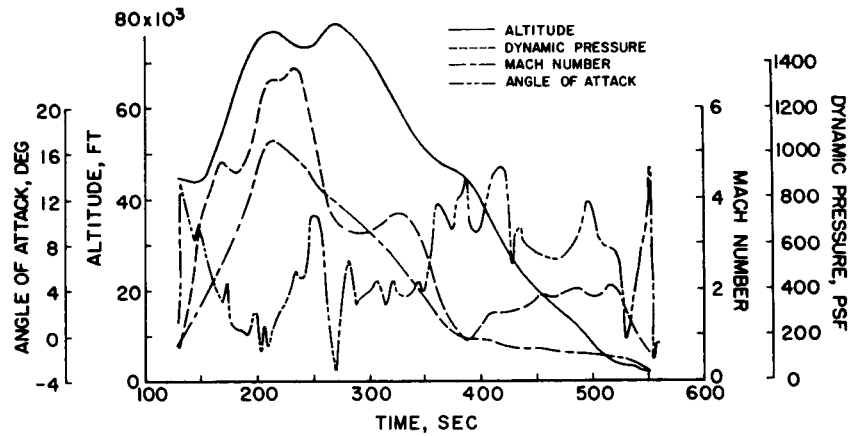


Figure 7

## OVERALL-SOUND-PRESSURE-LEVEL TIME HISTORY

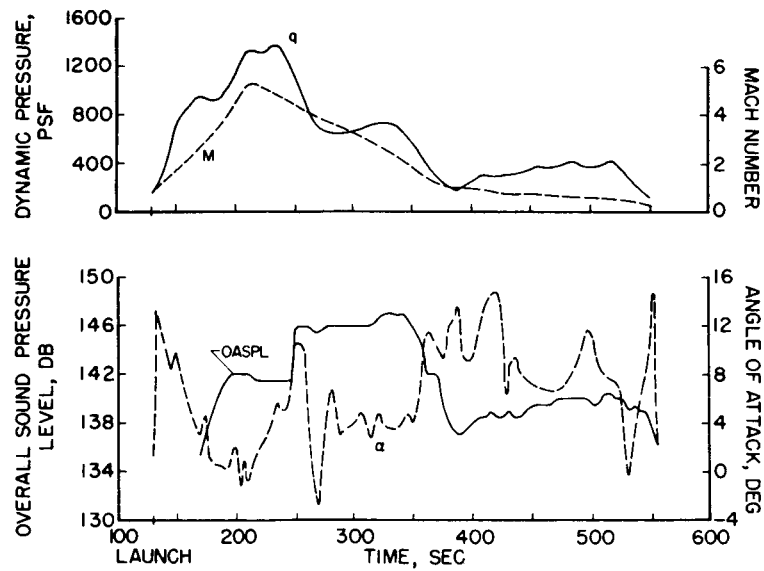


Figure 8

# BOUNDARY-LAYER-NOISE SPECTRA

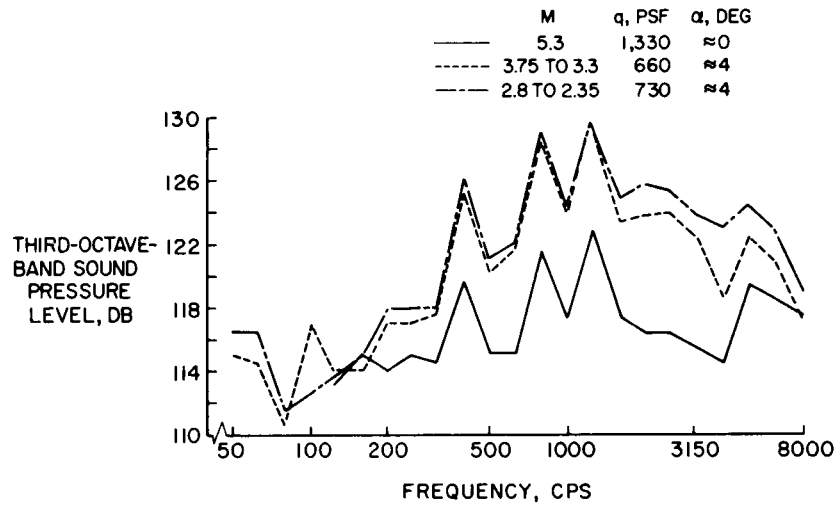


Figure 9

# NORMALIZED BOUNDARY-LAYER PROFILES

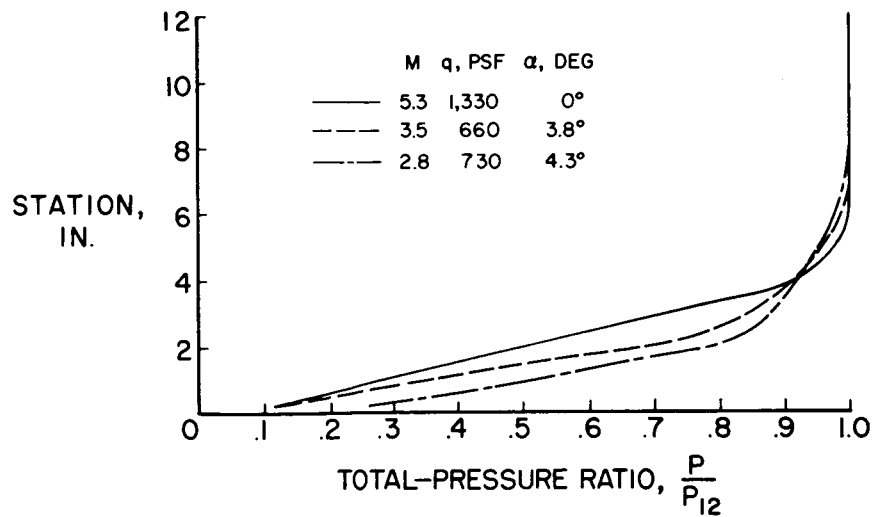


Figure 10

## SURFACE-PRESSURE COEFFICIENT AS FUNCTION OF MACH NUMBER

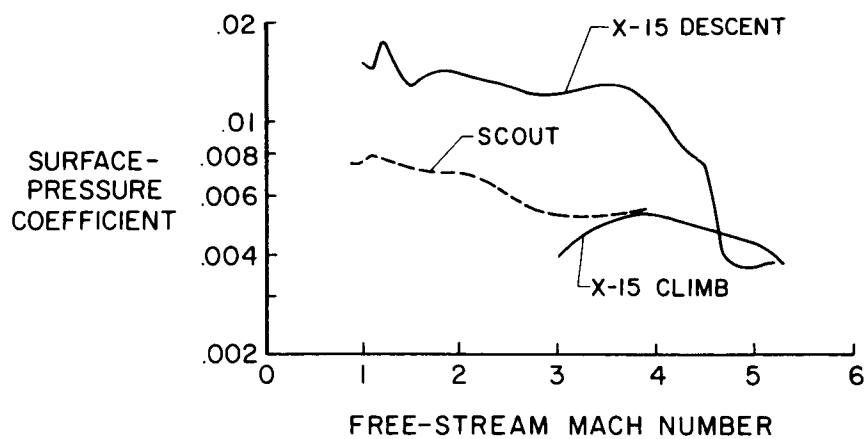


Figure 11